

Induction motor bearing fault analysis using Root-MUSIC method

Ahmed Hamida BOUDINAR, *Member, IEEE*, Noureddine BENOZZA,
Azeddine BENDIABDELLAH, *Member, IEEE*, Mohammed KHODJA
Electrical Engineering Faculty, Diagnosis Group
University of Sciences and Technology of Oran
Oran, Algeria

Abstract – This paper describes a new diagnosis approach, the Root-MUSIC (RM) method, for identification of the progressive cracking in the bearing of induction motors. This approach has several advantages compared to the stator current spectral analysis using the conventional Periodogram method. Indeed, the main advantage of this approach is its very good frequency resolution for a very short acquisition time, something impossible to achieve with the conventional method. However, in order to reduce the computation time which is the main drawback of the RM method, this method will be applied to only a specified frequency band; one that carries information about the sought fault. Experimental results show the effectiveness of RM method on the reliability of the incipient bearing fault detection.

Keywords: *Bearing; Cracks; Frequency band; Induction motor; PSD; Root-MUSIC; Spectral analysis; Stator current.*

I. INTRODUCTION

The induction motor is the most common electric machine in the industry. Its main advantage is the absence of sliding electrical contacts, which leads to a simple and robust structure easy to build with low cost. However, various faults can appear on the induction motor making the fault detection procedure necessary to prevent the interruption of the industrial process. Several reliability studies conducted on a large number of induction motors, show that the bearing faults account for 52% of all failures. For that, early detection of bearing faults increases the life of the motors and thus avoids unnecessary financial losses [1-3]. To identify these faults, several methods have been elaborated. Amongst the existing analysis methods, the Power Spectral Density estimation (PSD) by Periodogram of the stator current, is considered as a very popular technique and is widely used in industry. Several studies [4-8] have demonstrated the reasons for its durability in the field of diagnosis and its preference to other recent methods. The main reasons are:

- Easy programming.
- Easy implementation (microcontroller or FPGA).
- Fast computation time.

However, this method presents two major drawbacks:

- Frequency resolution conditioned by the acquisition time: Indeed, in order to have an efficient diagnosis, we must increase the acquisition time to be able to distinguish two close harmonics from each other.
- Identification for low harmonics quasi impossible [4]-[6]: Indeed, the presence of side-lobes related to the type of the window function used in the PSD estimation by Periodogram [5] risks masking the frequency signatures of incipient faults. Hence the importance of the adequate choice of this window.

Unfortunately, even an adequate choice of this window does not improve the diagnosis for certain operating modes of the motor, such as the rotor faults diagnosis at very low load. Indeed, in this case, the incipient fault signature is embedded in that of the fundamental. To eliminate this effect from the fundamental, some studies use the combined information found in the current and voltage, in order to calculate the instantaneous power [9-10]. However, this solution is not always accurate and, in addition, it is expensive, because it requires the use of sensors of currents and voltages.

For this reason, many researchers have focused their work towards using the Hilbert method to avoid fundamental effect on the analysis of the current spectrum and avoid the problem of the choice of the window function [11-12]. The Hilbert method is certainly suitable for diagnosis of rotor faults, but it is not very effective for other types of faults. Moreover, both approaches are unable to distinguish two close harmonics from each other with a very short acquisition time. That means a mediocre frequency resolution. To improve this resolution frequency and therefore the diagnosis reliability, in recent years, several advanced signal processing methods such as High Resolution Spectral Analysis have been applied to diagnose induction motor faults. These methods, as MUSIC [4], [6] and [13] and ESPRIT [14-15], use the decomposition of the covariance matrix of the signal analyzed in two separate subspaces: signal subspace and noise subspace. They are more robust to noise but require an important computation time, due to the complexity of their algorithms. On other hand, the PRONY method [16], which is not based on the decomposition of space, is faster compared to MUSIC, but more sensitive to measurement noise.

Note that all these methods that we have just mentioned are inappropriate in the case of a signal analysis in the presence of a speed variation or load change. Indeed, for these two operating modes, signals are non-stationary and therefore require the use of other methods such as time-frequency methods and time-scale methods.

For the time-frequency methods, the most common approach because easy to program, is the Short Time Fourier Transform (STFT) [17-18]. This method allows monitoring the useful information of the signal depending on the speed variation for example. However its main disadvantage is its low resolution time-frequency. In the same family, another method based on the Wigner-Ville Distribution (WVD) [19] improves time-frequency resolution at the expense of the appearance of interference terms or cross terms around the frequencies of the signal, mainly due to noise contained in this signal. These cross terms can be mitigated by eliminating the noise effects thanks to a variant of the WVD called Smoothed Pseudo Wigner-Ville Distribution (SPWVD) [20]. Unfortunately, this procedure causes a relocation of frequencies, key parameter in the faults diagnosis. Finally among the time-scale methods, the most known method is undoubtedly, that based on the wavelet transform [21-24]. This method is very effective in the case of change of speed or load, but its major drawback is the complexity of interpreting the resulting spectra and the long computation time, in addition to the importance of the choice of the used wavelet.

In this paper, we are interested in fault diagnosis of induction motor bearings, operating at constant load and constant speed, by using a variant of the MUSIC method (Multiple Signal Classification), namely the Root-MUSIC method. Yet, the disadvantage of this method is the long computation time required for the motor diagnosis. In fact, if the model orders (that is the number of sought harmonics) and/or the number of used samples are important this will lead to an increase of the used memory size and consequently to an increase of the computation time.

Furthermore, we know that the signature of each type of faults is localized in a well specified frequency band of the stator current spectral [4]-[6]. Hence, the basic idea we are proposing in this paper, consists of not applying the *RM* method in the complete stator current spectrum, but only within certain frequencies bands susceptible to inform us on the presence or not of the sought faults in the motor. This will enable us to reduce the used memory space and consequently the computation time [4], [6]-[13]. From this fact, the experimental results obtained with this approach will be compared to the *PSD* classical method to illustrate the merits of this proposed method.

II. STATOR CURRENT SPECTRUM CONTENTS

The application of the proposed Root-MUSIC method requires, like all spectral analysis methods regardless of the technique used (the current or the vibration), prior knowledge of the bearing dimensions to diagnose, in order to locate and interpret the frequency signature of sought fault.

For this purpose, it should be known that the rolling-element bearings act as an electromechanical interface between the stator and the rotor. In addition, they represent the holding element from the axis of the machine to ensure proper rotation of the rotor. The bearings are constituted by two races, the inner race and the outer race, balls and the cage which ensures equidistance between the balls as is shown in Fig. 1 [25].

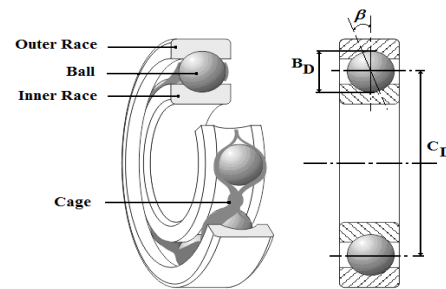


Fig. 1. Geometry of a rolling-element bearing.

Failures may affect the bearing on both races, on the ball or on the cage. Several studies have shown that the failure of each bearing element is manifested by a vibrational frequency characterizing the fault type [25-26].

- Characteristic frequency of the outer race fault

$$f_o = \frac{N_b}{2} f_r \left(1 - \frac{B_D}{C_D} \cos \beta \right) \quad (1)$$

- Characteristic frequency of the inner race fault

$$f_i = \frac{N_b}{2} f_r \left(1 + \frac{B_D}{C_D} \cos \beta \right) \quad (2)$$

- Characteristic frequency of the ball fault

$$f_{ball} = \frac{C_D}{B_D} f_r \left(1 - \frac{B_D^2}{C_D^2} \cos^2 \beta \right) \quad (3)$$

- Characteristic frequency of the cage fault

$$f_{cage} = \frac{1}{2} f_r \left(1 - \frac{B_D}{C_D} \cos \beta \right) \quad (4)$$

Where N_b is the number of bearing balls, B_D and C_D are the ball and the cage diameter respectively, β the contact angle and f_r the mechanical rotor frequency.

Furthermore, Schoen showed in [26] that bearing faults signatures appear in the stator current spectrum at the following frequencies:

$$f_{bear} (Hz) = |f_s \pm k \cdot f_v| \quad \text{with } k = 1, 2, 3, \dots \quad (5)$$

Where f_s is the supply frequency and f_v the fault characteristic frequency (f_o, f_i, f_{cage} or f_{ball})

It should be noted, that a preliminary calculation of these frequencies allows an optimization of the fault diagnosis of bearings because it enables us to know in advance the frequency bands where the fault signature is likely to appear.

III. ROOT-MUSIC METHOD

A. Data Model

The RM method is defined as a high resolution method. It is a variant of the Multiple Signal Classification (MUSIC) [4], [6]-[27]. This method assumes that the discrete-time signal $i_s(n)$ can be represented by L complex sinusoids in a noise $w(n)$, as follows:

$$i_s(n) = \sum_{i=1}^L I_i \cdot e^{j(2\pi \frac{f_i}{f_{sf}} n + \phi_i)} + w(n); \quad n=0, 1, \dots, N-1 \quad (6)$$

Where f_{sf} is the sampling frequency, N is the sampling number. I_i , f_i , ϕ_i represent the amplitude, frequency, and initial phase angle of the i^{th} harmonic respectively, $w(n)$ is a white noise. We note that (6) represents well the stator current model in the discrete time-domain.

B. Principle of Root-MUSIC method

The principle of this method also known as the subspace method is based on the Eigen decomposition of the autocorrelation matrix of the signal to be processed [4], [6], [16]-[27]. The estimated autocorrelation matrix R_i of measurement signal $i_s(n)$, represented by (7), is the sum of two autocorrelation matrices, these are the signal matrix R_s and the noise matrix R_w .

$$R_i = R_s + R_w = S.A.S^H + \sigma_w^2.I \quad (7)$$

- S is the Vandermonde matrix: $S = [s_1 \dots s_i \dots s_L]$

$$\text{with } s_i = \begin{bmatrix} 1 & e^{j.2\pi \frac{f_i}{f_{sf}}} & e^{j.4\pi \frac{f_i}{f_{sf}}} & \dots & e^{j.2\pi \frac{f_i}{f_{sf}}(N-1)} \end{bmatrix}^T \quad (8)$$

- A is the powers matrix of harmonics.

$$A = \text{diag}[I_1^2 \quad I_2^2 \quad \dots \quad I_L^2] \quad (9)$$

- H represents the Hermitian operator. σ_w^2 , and I are the noise variance of the white noise and the identity matrix of size $(N \times N)$ respectively.

The Eigen decomposition of the autocorrelation matrix of the signal R_i is given by the following relation [6]:

$$R_i = \sum_{k=1}^N \lambda_k \cdot u_k \cdot u_k^H = \underbrace{U_s \cdot D_s \cdot U_s^H}_{R_s} + \underbrace{U_w \cdot D_w \cdot U_w^H}_{R_w} \quad (10)$$

Where the matrices U_s and U_w are composed by the Eigen vectors u_k related to Eigen values arranged in descending order λ_k . The matrices D_s and D_w are diagonal matrices made by Eigen values λ_k .

$$\begin{aligned} U_s &= [u_1 \dots u_L]; \quad D_s = \text{diag}[\lambda_1 \dots \lambda_L] \\ U_w &= [u_{L+1} \dots u_N]; \quad D_w = \sigma_w^2 \cdot I_{N-L} \end{aligned} \quad (11)$$

Equations (10) and (11) show that, we can divide the global space into two groups or subspaces [6]:

- Signal subspace: composed of the Eigen values corresponding to the L largest Eigen values.

- Noise subspace: composed of the Eigen values corresponding to the $N-L$ remaining Eigen values.

Theoretically, all Eigen values corresponding to the noise subspace are equal to σ_w^2 . For this reason, D_w is written in the form given by (11). By comparing (7), (10) and (11) we can write:

$$R_i \cdot U_w = S.A.S^H \cdot U_w + \sigma_w^2 \cdot U_w \quad (12)$$

$$\text{This implies that: } S^H \cdot U_w = 0 \quad (13)$$

The problem comes down therefore to compute the solutions of (13). These solutions or roots appear accordingly on (or near) the unit circle. Unfortunately in reality, this is not too simple since the localization is not easy in the noise signal presence, because the roots corresponding to the sought frequencies are no more situated on the unit circle but mixed with the other solutions. To keep away the parasites roots from the unit circle and hence decrease the error probability, RM method considers that the whole set of the Eigen vectors are associated to the noise space E_w in order to obtain a better robustness with respect to the noise. We have therefore to solve the following equation [6], [15]-[27]:

$$s_i^H U_w \cdot U_w^H \cdot s_i = 0 \quad (14)$$

The phases of the L closest roots to the unit circle will correspond to the sought frequencies. These frequencies will be computed directly from the following relation [6]:

$$f_i = \frac{f_{sf}}{2\pi} \cdot \text{arg}(e^{j.2\pi \frac{f_i}{f_{sf}}}) \quad \text{with } i=1, \dots, L \quad (15)$$

Knowing the frequencies of the sought harmonics, we can therefore determine the amplitudes of these components by using the following equation:

$$R_s = S.A.S^H = \sum_{k=1}^L (\lambda_k + \sigma_w^2) u_k \cdot u_k^H \quad (16)$$

We notice that it is easier to inverse R_s rather than to inverse S . In these conditions, the amplitudes are estimated by [4], [6]:

$$A^{-1} = \frac{I}{S^H R_s^{-1} S} \quad (17)$$

$$\text{Where: } \begin{cases} R_s^{-1} = \sum_{k=1}^L \frac{I}{\lambda_k + \sigma_w^2} u_k \cdot u_k^H \\ \sigma_w^2 = \frac{I}{N-L} \sum_{k=L+1}^N \lambda_k \end{cases} \quad (18)$$

IV. IMPROVEMENTS OF THE ROOT-MUSIC METHOD

The major drawbacks of RM method are [4], [27]:

- The computation time which is very important and that increases with the samples number and the model order L . Note that in our paper, L represents the sought faults.
- The number of the sought harmonics estimation (L).

To solve these drawbacks, we propose the following solutions:

A. First Solution:

Several studies have demonstrated that the signature of each type of faults are localized on a well precise frequency band of the stator current spectrum; the suggested idea consists therefore in processing the data on a given frequency band and not on all the spectrum of the stator current. This solution will hence enable us to reduce the length of the spectrum and consequently will reduce the computation time [4], [6]-[13].

Hence, *RM* method will be applied solely to a frequency band defined by a low cut-off frequency f_l and a high cut-off frequency f_h . These cutoff frequencies will be selected on the spectrum width $[0, f_{sf}/2]$, depending on the type of the studied fault. With this solution, the processing will be done on $2.N.f_p / f_{sf}$ samples where $f_p = f_h - f_l$ and not on the N samples, these reducing the computation time.

To confirm the positive contribution of this solution with respect to the computation time, several tests have been carried out [4], [6]. Thus, on the basis of several new tests, the computation time is equal to 147.53 s for the fundamental identification only ($L=1$), with the original Root-MUSIC method, see Table I. Note that we obtained these results by considering a signal of 10000 samples and using a PC equipped with a dual-core processor of 2 GHz and 3 GB of RAM.

TABLE I
SPEED COMPUTATION COMPARISON

Method	Data length	Fundamental Identification (Frequency / Magnitude)	Computation time (s)
Original Root-MUSIC	10000	50.003 Hz / 16.44 dB	147.53
Improved Root-MUSIC	136	50.004 Hz / 16.15 dB	0.4

Unfortunately if the size of the signal increases a hundred thousand samples, then the computation time quickly becomes prohibitive. This problem occurs because of the roots calculation (see equation (14)) and the matrix inversion (see equation (17)). This problem becomes even more complex, if the number of the sought harmonics (L) is higher.

By cons, our solution, which is to seek the desired harmonics only within a defined band, avoids this problem. In fact, Table I shows that the improved Root-MUSIC allows to reduce the data length (136 samples) and the computation time (0.4 s) by considering an analysis band [40 Hz 60 Hz] for the identification of the fundamental ($L = 1$).

B. Second Solution:

The *RM* performances can be completely deteriorated by choosing a wrong value of the model order L . In fact, if L is too small, then we can lose the harmonics of low amplitudes. By cons, if L is too large, then the spectrum may contain spurious harmonics. To determine this parameter, various estimation criterions have been developed [6], [27-28].

As a solution, we propose in this paper to set the number of the sought harmonics to 1 ($L = 1$). In fact, the proper selection

of the frequency band to be processed, enables the identification of a single harmonic, that of the sought fault.

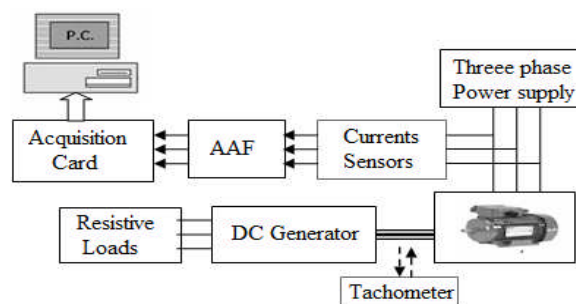
The next procedure describes the steps to follow for the analysis and processing of the phase stator current using the proposed approach:

1. Acquisition of the phase current.
2. Determination of the processed frequency band, the band which is likely to show the signature of the sought fault.
3. Choice of the sought harmonics number (in this paper, $L=1$).
4. Application of the Root-MUSIC to the $2.N.f_p/f_{sf}$ samples.
5. Verification if the localized frequency corresponds to that obtained by calculation.

V. EXPERIMENTAL RESULTS

A. Test rig and acquisition parameters

The main experimental tests that are being presented in this paper are carried out by the diagnosis group in the laboratory of development of electrical drives “LDEE”. The motor used in the experimental investigation is a three-phase squirrel cage motor coupled to a DC generator. The motor parameters are: 3kW, 1410 rpm, 50Hz, 4 poles. The measuring system includes two current Hall Effect sensors (Fluck i30s), an anti-aliasing filter *AAF* (realized in our laboratory) with a 400 Hz adjustable cut-off frequency chosen for our tests, and an acquisition card (NI-6330). The whole set is connected to a computer for viewing the processed sensed signal as shown in Fig. 2. In addition, a tachometer (Ono Sokki HT-341) is used for measuring the actual shaft speed of the motor.



a. Synoptic diagram of test rig



b. Photo of test rig

Fig. 2. Realised test rig

All acquisitions were performed at 1440 rpm and in steady state. The acquisition time is of 40 seconds, with a sampling frequency of 3 KHz. In these conditions, the signal length is equal to 120000 samples and the frequency resolution is equal to 0.025 Hz.

The bearing in the motor to be diagnosed is of ball bearing type of reference 6205-ZZ “opposite side to coupling”. The bearing specifications are: $B_D=7.835$ mm, $C_D=38.5$ mm, $N_b=9$ and $\beta=0$. Fig. 3 illustrates the faults created in the bearings used in our experimental tests.

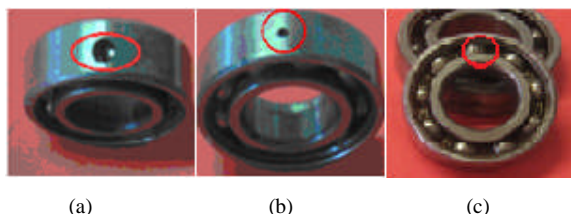


Fig.3. Artificial bearing faults. (a) and (b) Outer race fault (6mm and 3mm holes), (c) Cage and ball fault.

The bearing faults dealt with are artificially created by the Electrical Discharge Machining “EDM” in order to simulate the same situations as real ones. The holes dimensions are 6mm and 3mm in diameter and 2.5 mm in depth.

In this paper, we consider the hole of 03 mm diameter as an incipient fault:

- Compared with other holes and grooves made on other bearings in our laboratory “for example 6mm diameter holes, breaks in the cage on 4mm, grooves on the outer ring 3mm across its width etc.”
- But, essentially, on the fact that the classical method of the PSD estimation by the periodogram technique, widely used in industry, is unable to detect any frequency signature of this hole of 03 mm diameter and of 2.5 mm depth, as we shall see it thereafter in this paper.

The various modes of operation performed to validate the diagnostic procedure are:

- Motor operation with healthy bearings,
- Motor operation with outer race fault (6 and 3 mm holes)
- Motor operation with cage fault,
- Motor operation with cage and balls faults

For a more reliable analysis and due to the randomness of the measured signals, several acquisitions were made for each operation.

Theoretically, the frequencies signatures of an outer race, cage and balls faults are determined by the geometric parameters of the bearing based on (1), (3), (4) and (5). The following table shows the frequencies signatures of each fault that may appear on the current spectrum at 1440 rpm ($f_r=24$ Hz).

TABLE II
THEORETICAL BEARING FAULTS FREQUENCIES AT 1440 RPM AND K=1

<i>Faults frequencies</i>	<i>Lower sideband:</i> $f_{bear}(Hz) = f_s - f_v$	<i>Upper sideband:</i> $f_{bear}(Hz) = f_s + f_v$
Outer race fault	36.02 Hz	136.02 Hz
Cage fault	40.44 Hz	59.55 Hz
Balls fault	63.04 Hz	163.04 Hz

Knowing the theoretical frequency position of the bearing faults dealt with in this paper (see Table II), it is also necessary to choose properly the frequency bands to be analyzed, to detect experimentally these faults signatures. The choice of these bands must take into account possible variations of the load. Indeed, any load variation affects the mechanical frequency measured which affects of course the frequency positions of the bearing faults. The following two tables show the two extreme cases of the operating motor at very low load and overload.

TABLE III
THEORETICAL BEARING FAULTS FREQUENCIES AT OVERLOAD:
MOTOR SLIP 7% “ 23.25 Hz” AND K=1

<i>Faults frequencies</i>	<i>Lower sideband:</i> $f_{bear}(Hz) = f_s - f_v$	<i>Upper sideband:</i> $f_{bear}(Hz) = f_s + f_v$
Outer race fault	33.33 Hz	133.33 Hz
Cage fault	40.74 Hz	59.25 Hz
Balls fault	59.51 Hz	159.51 Hz

TABLE IV
THEORETICAL BEARING FAULTS FREQUENCIES AT VERY LOW LOAD:
MOTOR SLIP 1% “ 24.75 Hz” AND K=1

<i>Faults frequencies</i>	<i>Lower sideband:</i> $f_{bear}(Hz) = f_s - f_v$	<i>Upper sideband:</i> $f_{bear}(Hz) = f_s + f_v$
Outer race fault	38.70 Hz	138.70 Hz
Cage fault	40.14 Hz	59.85 Hz
Balls fault	66.58 Hz	166.58 Hz

Based on the tables (III) and (IV), if we are interested in tracking faults harmonics according to the “lower sideband” then we will choose the following frequencies bands analysis:

- [30 Hz, 45 Hz] to search for the outer ring faults and the cage faults.
- [55 Hz, 70 Hz] to search for the balls faults.

If by cons, we are interested in monitoring faults harmonics according to the “upper sideband”, then we must choose the following frequencies bands analysis:

- [130 Hz, 145 Hz] to search for the outer ring faults.
- [55 Hz, 70 Hz] to search for the cage faults.
- [155Hz, 170 Hz] to search for the balls faults.

Note that the choice of these frequencies bands takes into account the entire range of possible load variations to enable the diagnosis of the three types of faults treated. In addition, by choosing these frequencies bands, we avoid the known strong harmonics such as slot harmonics, third harmonic or the fundamental that can hide the sought fault harmonic. Thus, in this paper, we have chosen the lower sideband for these bearing faults diagnosis.

In this paper, we analyzed only the first Lower Sideband (for $k = 1$). We would have been able to also choose to analyze the first Upper Sideband (for $k = 1$). As we can also analyze other bands ($k = 2, 3 \dots$). The choice of the band does not affect diagnostic reliability knowing that the frequency signature of the bearing fault appears on the entire current spectrum depending on the chosen variable k (see (5)).

B. Motor operation with healthy bearings

In these first tests, we will analyze the stator current in the case where the two bearings “the opposite side to coupling and the coupling side” are healthy.

To note, what we call healthy bearing in this paper, it is a bearing that does not present any visually apparent faults. This does not exclude the existence of imperfections related to either its manufacturing phase or to the existence of scratches associated with its use.

This first identification step is very important and necessary, because all the next set of tests are going to be compared to that first identification step known as ‘the reference step’. Fig. 4 shows the results obtained by the classical *PSD* at 1440 rpm. We can notice that except the fundamental, no other significant harmonic appears on the two selected frequencies bands.

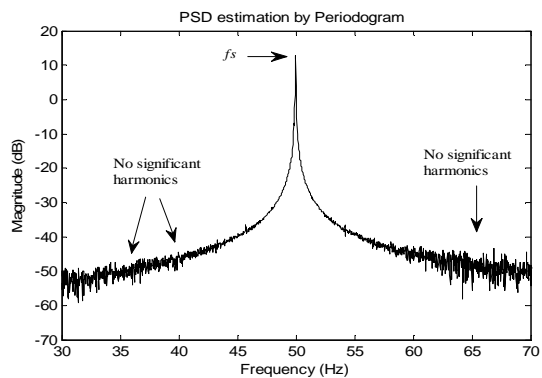


Fig.4. Stator current analysis by classical *PSD* method - Healthy bearings-

In the light of these first results, we remark that there is no particular harmonic presence in the spectrum this confirms that our bearings are healthy.

By cons, by analyzing the stator current with improved *RM* method, we note that on the first frequency band (Fig.5.a), the appearance of a harmonic of frequency 36.59 Hz and magnitude -36.97 dB.

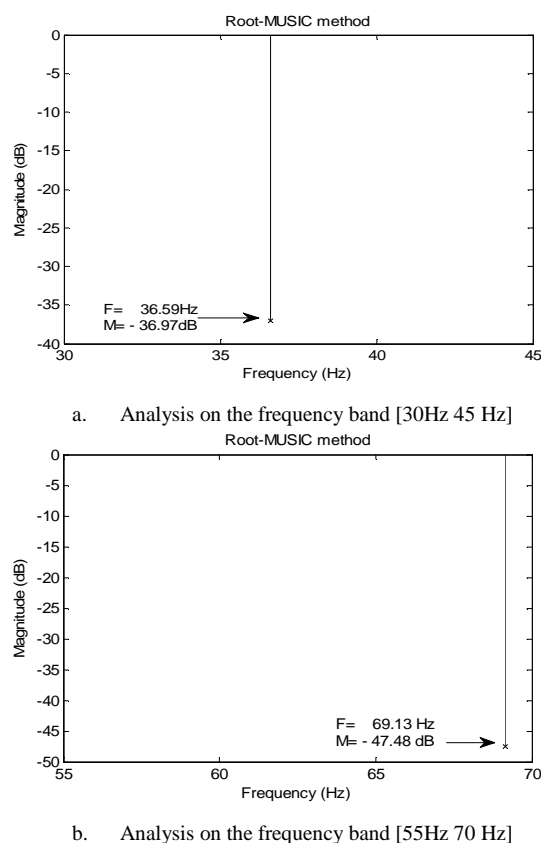


Fig.5. Stator current analysis by *RM* method - healthy bearings-

Comparing this result with Table II, we can suppose that this harmonic represents an anomaly or a simple scratch on the outer race of the bearing, supposed to be healthy ". The presence of this scratch can be explained by the repetitive process of the assembly/disassembly of the bearing during the various tests (several dozen experiments carried with the same bearing). Indeed, the outer race is the part of the bearing which is most exposed to a failure with regard to its geometrical position. This scratch can be also considered to be an incipient fault.

Furthermore, on the second frequency band (Fig.5.b), there is the appearance of a harmonic of frequency 69.13 Hz. The existence of this harmonic is due to the number L chosen for our algorithm. This harmonic can be considered insignificant given its magnitude (-47.48 dB).

C. Motor operation with outer race fault

In this second set of tests. Fig.6 represents graphically the obtained experimental results by the classical *PSD* method for the case of an outer race fault. According to table II, the harmonic characterizing the fault of the outer race should appear at a frequency of 36.02 Hz, which is on the first selected frequency band.

According to Fig. 6.a, we find that this method shows a very low harmonic at 36.6 Hz, in the case of a 6 mm hole on the outer race of the bearing. Fig. 6.b shows that the conventional method of the *PSD* is unable to identify the frequency signature of sought fault.

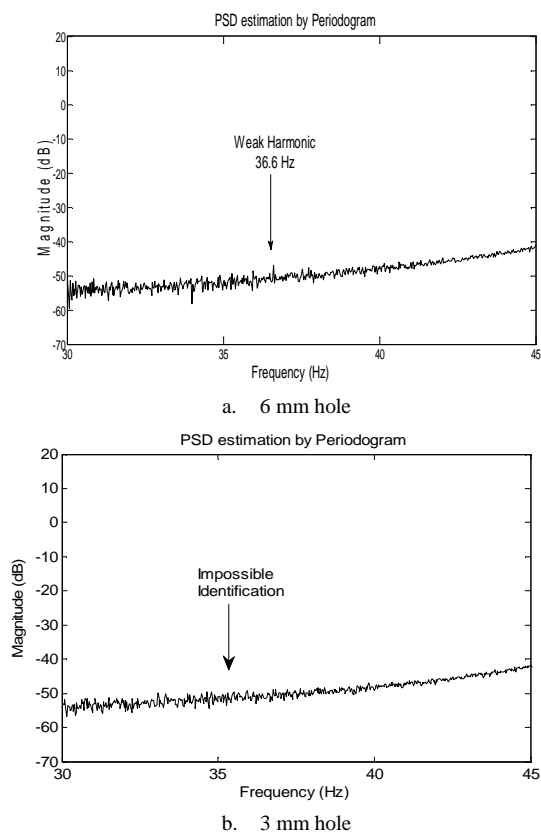


Fig.6. Stator current analysis by classical *PSD* method - Outer race fault -

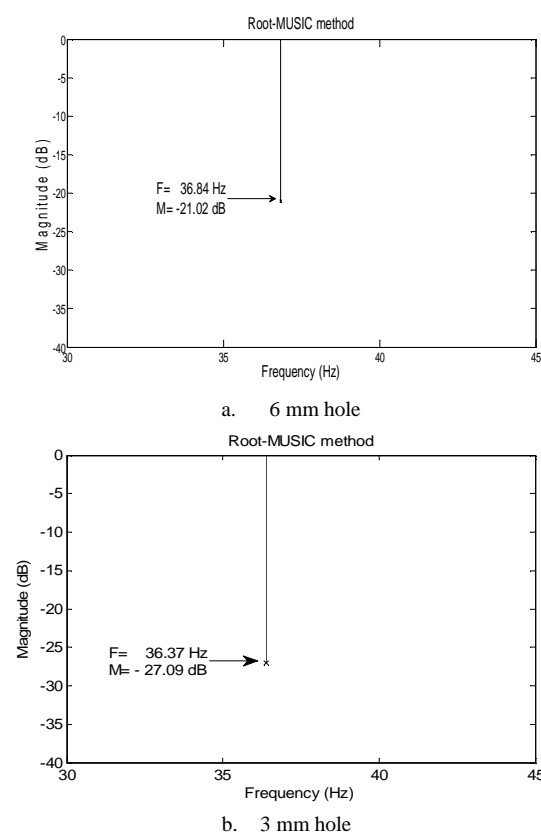


Fig.7. Stator current analysis by *RM* method - Outer race fault -

Otherwise, the *RM* method can identify the frequency signature of the sought fault, namely 36.84 Hz for the case of a 6mm hole and 36.37 Hz for the case of a 3mm hole as shown in Fig.7. Note that this slight difference between the theoretical frequency (36.02 Hz) and those obtained (36.84 Hz and 36.37 Hz) is probably linked to a slight variation of the motor mechanical speed. Furthermore, the assumption we made about the existence of an early crack of the outer race (see section V.B) is justified since the magnitude of this harmonic increases with the cases studied:

- Supposed healthy (36.59Hz, -36.97 dB) (see Fig.5.a)
- A 3mm hole (36.37 Hz, -27.09 dB) (see Fig.7.b)
- A 6mm hole (36.84Hz, -21.02 dB) (see Fig.7.a).

In the light of these results, we can say that Root-MUSIC with the proposed improvements, allows not only to detect incipient faults but especially to monitor their evolutions as shown in Fig. 8:

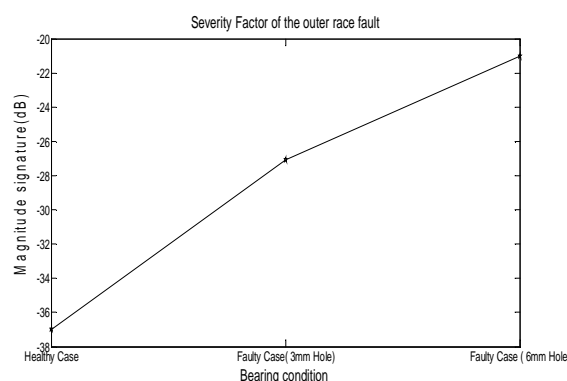


Fig.8. Severity Factor of the outer race fault

D. Motor operation with cage fault

The following figures represent graphically the obtained experimental results by both the classical *PSD* and *RM* methods for the case of a cage fault.

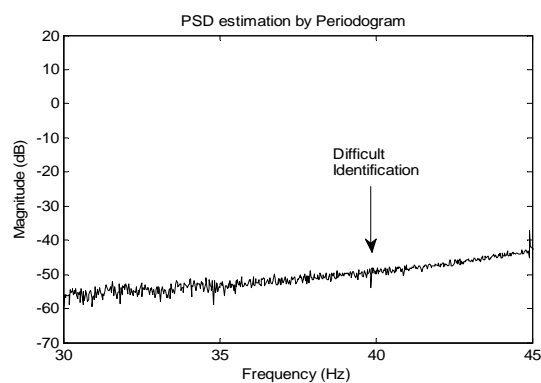


Fig.9. Stator current analysis by classical *PSD* method - Cage fault-

From Fig.9, we find that the classical method of the *PSD* by Periodogram is still unable to identify the frequency signature of the sought fault which is supposed to appear, according to Table II, at the frequency of 40.44 Hz. This result was predictable given the diameter of the hole.

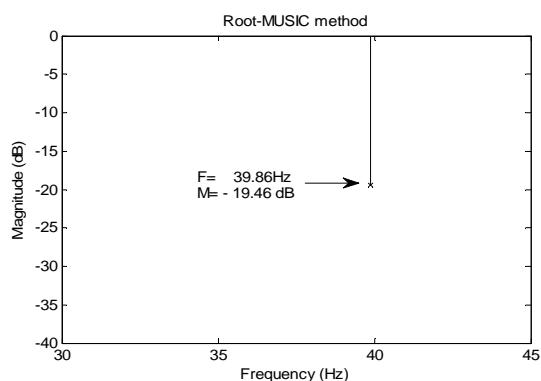


Fig.10. Stator current analysis by *RM* method - Cage fault-

Otherwise by using the *RM* method, see Fig.10, we can note that this technique arrives at estimating not only the sought harmonic over the specified frequency band but also exhibiting this harmonic in a very clear manner to be easily detectable (39.86 Hz).

E. Motor operation with cage and balls faults

In these last tests, we will see the effectiveness of the *RM* method with the proposed solutions in the case of a double fault: fault of the cage and the ball at the same time. From Fig. 11, we see that classical *PSD* method is unable to diagnose the two types of faults on the two selected frequencies bands (Fig.11.a and Fig.11.b). Again, this finding was predictable given the size of the holes made.

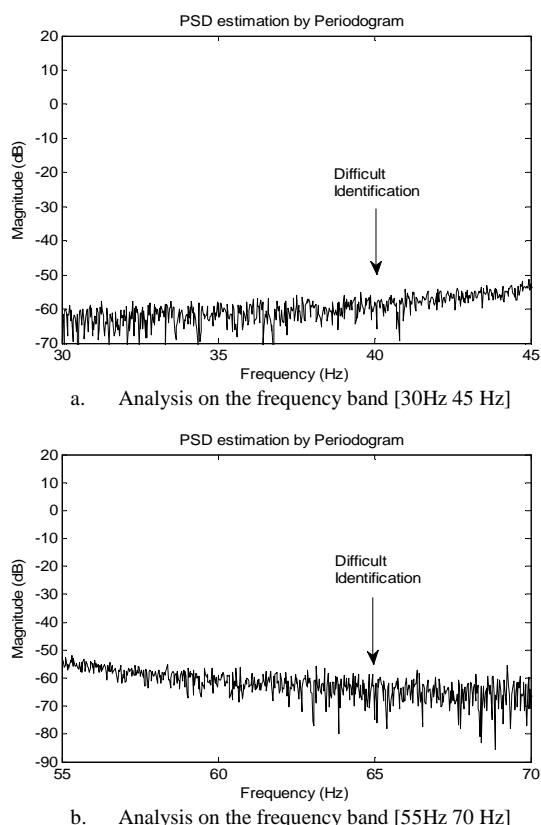
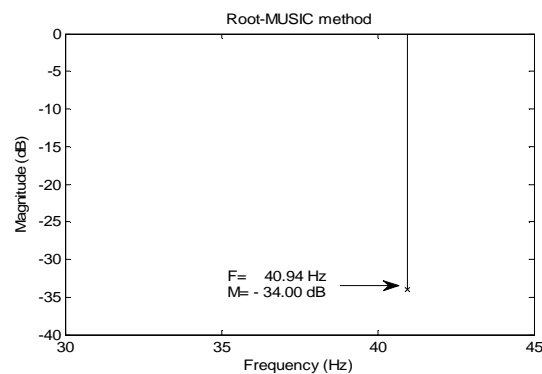
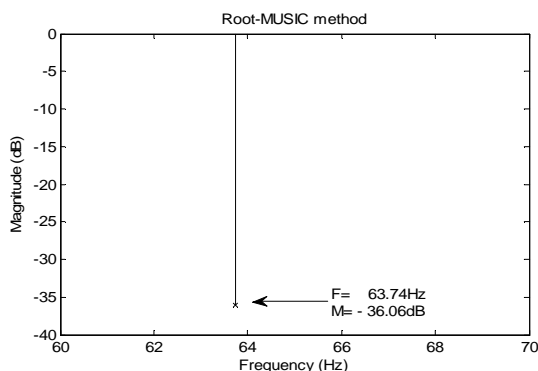


Fig.11. Stator current analysis by classical *PSD* method - Cage and Balls faults-



a. Analysis on the frequency band [30Hz 45 Hz]



b. Analysis on the frequency band [55Hz 70 Hz]

Fig.12. Stator current analysis by *RM* method - Cage and Balls faults-

Fig. 12 shows us the sought harmonics over the specified frequencies bands (Fig12.a and Fig12.b) by using the *RM* method. We notice that these harmonics reflect well the cage and ball faults presence in comparison to the obtained theoretical frequencies (see table II).

In fact, Fig. 12.a shows the frequency signature of the cage fault (40.94 Hz), and the Fig. 12.b gives us the signature of the balls fault (63.74 Hz). This slight difference between the theoretical values and that obtained is certainly due to the error on the measurement of the mechanical speed by the tachometer or to a slight variation of the motor mechanical speed.

We notice again, that the obtained results by the use of the *RM* method are very exploitable. In fact, we can easily note that this technique presents a very good identification (good estimation of frequencies and magnitudes) of all the sought harmonics over the specified frequencies bands.

In the light of the results obtained, we can say that this method can be applied to real cases, provided to properly define the frequency band to be analyzed which likely shows the frequency signature of the sought fault. Because it is well known that each fault has a particular signature localized at a particular frequency.

Finally, we can mention another advantage of the improved Root-MUSIC compared to the classical method of the *PSD* estimation by the Periodogram technique aside from the frequency resolution and the spectrum clarity. Indeed, the classical method gives a spectral expanded, and it is the user who has to search the frequency signature representing the

existing faults. By cons, with our approach, we define the frequency band to analyze according to the type of the sought fault, that which is easier and faster, in our opinion. Moreover, if we look for several types of faults at the same time, we have only to define several frequencies bands to analyze according to possible frequency position of the sought fault.

VI. CONCLUSION

In this paper, we prove that the classical *PSD* method by Periodogram allows a fast harmonics estimation; but it does not allow the detection of low magnitude faults such as incipient fault. However, the obtained sets of results based on experimental data, clearly indicate that the *Root-MUSIC* method has better discrimination capability and is more robust compared to the classical *PSD* method. The proposed solution in this paper, and which consists of treating only the frequency band likely to reveal the signature of the sought fault, has made the *Root-MUSIC* method faster and more efficient.

This method has positively contributed in the readability of the stator current spectrum and significantly facilitated its analysis. Also, this method has enabled us to verify the correlation between the frequency signatures of the bearing faults obtained experimentally and those calculated theoretically. These results also prove that the improved *Root-MUSIC* method is very effective not only to detect the incipient faults, but also to monitor the evolution of the faults severity

REFERENCES

- [1] H. A. Toliyat, S. Nandi, S. Choi, H. Meshgin-Kelm, "Electric machines: Modeling, condition monitoring and fault diagnosis," Taylor & Francis Group Eds. New York, 2012, pp. 1-23.
- [2] O. V. Thorsen and M. Dalva, "Failure identification and analysis for high voltage induction motors in the petrochemical industry," IEEE Trans. Ind. Appl., vol. 35, no. 4, pp. 810-818, Jul/Aug 1999.
- [3] A. Garcia-Perez, R. Romero-Troncoso, E. Cabal-Yepez, R.A. Osornio-Rios, "The Application of High-Resolution Spectral Analysis for Identifying Multiple Combined Faults in Induction Motors," IEEE Trans.Ind. Elect., vol. 58, pp. 2002-2011, May 2011
- [4] A.H. Boudinar, A. Bendiabdellah N. Benouzza, N. Boughanmi, "Three phase induction motor incipient rotor's faults detection based on improved Root-MUSIC approach," International Review of Electrical Engineering, vol. 02, no.3, pp. 406-413. May/Jun. 2007
- [5] A.H. Boudinar, A. Bendiabdellah, N. Benouzza, M. Ferradj, "Improved stator current spectral analysis technique for bearing faults diagnosis," 16th International Power Electronics and Motion Control Conference and Exposition, Antalya, Turkey. 21-24 Sept. 2014
- [6] A.H. Boudinar, N. Benouzza, A. Bendiabdellah, , "Induction motor cracked rotor bars fault analysis using an improved Root-MUSIC method," 3rd International Conference on Control, Engineering and Information Technology (CEIT), Tlemcen, Algeria. 25-27 May. 2015
- [7] E. El Bouchikhi, V. Choqueuse, M.E.H. Benbouzid, "Current Frequency Spectral Subtraction and Its Contribution to Induction Machines' Bearings Condition Monitoring," IEEE Trans. Energ. Conv., vol. 28, no. 1, pp.135 – 144. Dec. 2012.
- [8] E. El Bouchikhi, V.Choqueuse, M.E.H. Benbouzid," Induction machine faults detection using stator current parametric spectral estimation". Mechanical Systems and Signal Processing, Elsevier, vol. 52-53, pp.447-464. Feb. 2014
- [9] A. Ibrahim, M.E. Badaoui, F. Guillet, F. Bonnardot, "A New Bearing Fault Detection Method in Induction Machines Based on Instantaneous Power Factor" IEEE Trans.Ind. Elect., vol. 55, no. 12, pp 4252-4259, Dec. 2008
- [10] A. Dzwonkowski, L. Swęrowski, "Uncertainty analysis of measuring system for instantaneous power research". Metrology and Measurement Systems. vol. 19 , no. 3, pp. 573-582, Sept 2012
- [11] Y. Amirat, V. Choqueuse, M.E.H Benbouzid, S. Turri "Hilbert Transform based bearing failure detection in DFIG-based wind turbines". International Review of Electrical Engineering, vol.6, no. 3, pp.1249-1256, 2011
- [12] A.G. Espinosa, J.A.Rosero, J. Cusido, L. Romeral, J.A.Ortega, "Fault detection by means of Hilbert–Huang Transform of the stator current in a PMSM with demagnetization". IEEE Trans. Energ. Conv., vol. 25, no. 2, June 2010
- [13] S.H. Kia, H. Henao, G.A Capolino, S.H. Kia, H. Henao, G.A Capolino, "A high-resolution frequency estimation method for three-phase induction machine fault detection," IEEE Trans.Ind. Elect., vol. 54, no. 4, pp. 2305-2314, Aug. 2007
- [14] Y.H.Kim et al, "High-Resolution Parameter Estimation Method to Identify Broken Rotor Bar Faults in Induction Motors," IEEE Trans. Ind. Elect., vol. 60, no. 9, pp.4103-4117 Sept. 2013.
- [15] B. Xu, L. Sun, L. Xu, and G. Xu, "Improvement of the hilbert method via esprit detecting rotor fault in induction motors at low slip". IEEE.Trans. Energ. Conv., vol. 28, no. 1, pp.225-233, Mar 2013.
- [16] M. Sahraoui, A.J.M Cardoso and A.Ghoggal, "The use of a modified prony method to track the broken rotor bar characteristic frequencies and amplitudes in three-phase induction motors," IEEE Trans. Ind. Appl., vol. 51, no. 3, May/June 2015.
- [17] A.F. Aïmer, A.H. Boudinar, N. Benouzza, A. Bendiabdellah, Simulation and Experimental Study of Induction Motor Broken Rotor Bars Fault Diagnosis using Stator Current Spectrogram, In Proc. of IEEE 3rd International Conference on Control, Engineering & Information Technology (CEIT), Tlemcen, Algeria. 25-27 May, 2015
- [18] E. El Ahmar, V. Choqueuse, M.E.H Benbouzid, Y. Amirat, J. El Assad. "Advanced Signal Processing Techniques for Fault Detection and Diagnosis in a Wind Turbine Induction Generator Drive Train: A Comparative Study". IEEE Energy Conversion Congress and Exposition (ECCE), Atlanta, United States. pp.3576 - 3581, 12-16 Sept 2010
- [19] V. Climente-Alarcon, J.A Antonino-Daviu, M. Riera-Guasp, M. Vlcek, "Induction motor diagnosis by advanced notch FIR filters and the Wigner–Ville Distribution". IEEE Trans.Ind. Elect., vol. 61, no. 8, pp 4217-4227, Aug 2013
- [20] H. Henao, G.A. Capolino, M.F. Cabanas, F.Fiupetti, C. Bruzzese, E. Strangas, R. Pusca, J. Estima, M. Riera-Guasp, S.H. Kia, "Trends in fault diagnosis for electric machines: A review of diagnostic methods" IEEE Ind. Elect. Magazines, vol.8, no.2, pp. 31-42, June 2014
- [21] R. Yan, R.X. Gao, X. Chen, "Wavelets for fault diagnosis of rotary machines: A review with applications". Signal Processing, Elsevier, vol. 96 Part.A, pp. 1-15, Mar 2014
- [22] J.P. Llinares, J.A. Antonino-Daviu, M.Riera-Guasp, M. Pineda-Sanchez, V. Climente-Alarcon, "Induction motor diagnosis based on a transient current analytic wavelet transform via frequency B-Splines." IEEE Trans.Ind. Elect., vol. 58, no. 5, pp. 1530-1544, Sept 2010.
- [23] A. Bouzida, O. Touhami, R. Ibtouen, A. Belouchrani, M. Fadel, A. Rezzoug, "Fault diagnosis in Industrial Induction machines through discrete Wavelet Transform." IEEE Trans.Ind. Elect., vol. 58, no. 9, pp. 4385-4395, Nov 2010
- [24] K.S. Gaeid, H.W Ping, "Wavelet fault diagnosis and tolerant of induction motor: A review." International Journal of the Physical Sciences. vol. 6 no 3, pp. 358-376, Feb. 2011
- [25] M. Blödt, P. Granjon, B. Raison, G. Rostaing, "Models for bearing damage detection in induction motors using stator current monitoring", IEEE International Symposium on Industrial Electronics ISIE 2004, Ajaccio, France.
- [26] R. Schoen, T. G. Habetler, F. Kamran, and R. G. Bartheld, "Motor bearing damage detection using stator current monitoring," IEEE Trans. Ind. Appl., vol. 31, no 6, pp 1274 – 279, Nov/Dec 1995.
- [27] M.H. Hayes, "Statistical digital signal processing and modelling," John Wiley & Sons, New-York, 1991.
- [28] S. Marcos, "Méthodes haute résolution," Hermes, Paris, 1998.